

Detecting 1st and 2nd Layer Simulated Cracks in Aircraft Wing Spanwise Splice Standards Using Remote-Field Eddy Current Technique

Yushi Sun, Tianhe Ouyang
Innovative Materials Testing Technologies, Inc.
2501 N. Loop Drive, Suite 1610, Ames, IA 50010
Robert J. Lord
Boeing-St. Louis, Engineer/Scientist 3
Nondestructive Evaluation - Phantom Works
St. Louis, MO 63166

ABSTRACT

There are a number of aging aircraft applications such as thick, multi-layer structure and 3-5 layer fuselage lap joints currently being inspected either visually or by manual NDI. The objective of this study was to evaluate advanced sensors to improve flaw sensitivity for large area scanning applications. The long-term goal is to integrate advanced sensor concepts with the Boeing-St. Louis's MAUS IV scanner. Eddy current devices utilizing the remote field eddy current (RFEC) effect have shown promise in inspecting for cracks through thick structure. An RFEC sensor, along with an RFEC system, developed by Innovative Materials Testing Technologies, Inc. was used to manually scan two aircraft wing-spanwise splice standards containing first and second layer slots in fastener holes. One standard had an aluminum wing skin/spar cap arrangement, each 0.125 inch thick and the total thickness is about 0.25 inch, whereas the other had an aluminum skin/spar cap that was each 0.25-inch thick and the total thickness was about 0.5 inch.

The test results show that the first and second layer slots in the two wing spanwise splice standards were detected using the RFEC technique.

INTRODUCTION

There are a number of aging aircraft applications such as thick, multi-layer structure and 3-5 layer fuselage lap joints currently being inspected either visually or by manual NDI. The detection of flaws that are located deep in such structures represents a major challenge. A number of different techniques have been proposed to address this problem. Examples of such NDE techniques include X-rays, ultrasonics, thermal wave imaging, magneto-optic imaging, single and multi-frequency eddy current, pulsed eddy current, eddy current self-nulling probes, superconducting quantum interface devices, high sensitivity magnetic sensors, such as magnetoresistive elements and giant magnetoresistive elements, remote-filed eddy current (RFEC) method, etc. Significant advances has been made in each of these techniques with respect to penetration depth, sensitivity and resolution in detecting corrosion and cracks in such structures. Among them, the RFEC technique has made significant strides during the last few years and shown promise in inspecting for cracks through thick structure. Recently Innovative Materials Testing Technologies, Inc. (IMTT) used an RFEC sensor, along with an RFEC system, to manually scan two aircraft wing spanwise splice standards containing first and second layer slots in fastener holes. One standard had an aluminum wing skin/spar cap arrangement, each

0.125 inch thick, whereas the other had an aluminum skin/spar cap that was each 0.25-inch thick. Boeing St. Louis provided the test panels and evaluated the test results.

The RFEC technique, first introduced for inspecting tubes, is characterized by its high sensitivity to anomalies at large depths. In addition, it offers equal sensitivity to an anomaly, irrespective of its location in the tube wall. When a coil excited by an alternating current is placed in a pipe as shown in Figure 1, the energy diffuses along two different paths. The interaction between the two fields results in what is often referred to as the remote field eddy current effect. Studies [1,2] indicate that the energy diffusing via the direct path attenuates very rapidly. The signal received by the pick-up coil that is located a certain distance away from the excitation coil is primarily due to the energy diffusing via the indirect path. This portion of the energy passes the pipe wall twice before arriving at the pick-up coil.

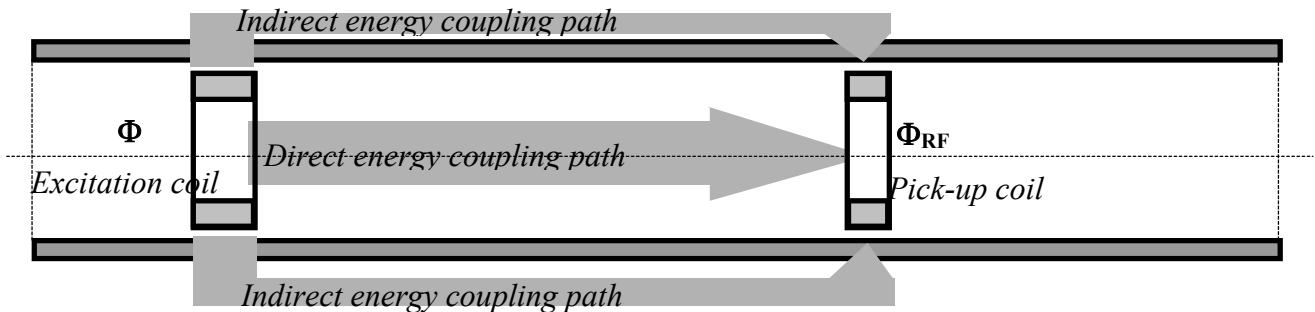


Figure 1. Remote field eddy current effect in a tube showing two paths of energy transmission

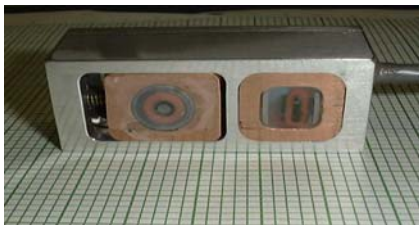


Figure 2. A typical prototype RFEC probe for inspecting thick aluminum plates

In recent years, the RFEC technique has been successfully extended to the inspection of metallic plates [3-4]. The key principle in designing such an RFEC probe involves the use of proper shielding to prevent the energy from the excitation coil from getting directly coupled to the sensor coil. Instead, the energy released by an excitation coil is focused to go through the test specimen. Experimental tests have shown that the RFEC system is capable of detecting deeply embedded flaws in thick and multi-layer metallic structures. A typical prototype RFEC probe designed for inspecting thick aluminum plates is shown in Figure 2.

MAJOR DIFFERENCES BETWEEN RFECT AND ECT

Conventional eddy current methods rely on the measurement of either the excitation coil impedance, Z , of an absolute or a differential probe, or the induced voltage, V_i , in the pick-up coil of a reflection probe. We know that the impedance value of a coil is approximately proportional to the total flux, Φ , linking the excitation coil. For reflection probes the induced voltage, V_i , is directly proportional to the flux, Φ_p , linking the pick-up coil. Traditionally in the case of an eddy current probe the pick-up coil is placed close to the excitation coil, and hence Φ_p should be proportional to Φ . The values of these two quantities should be of a similar order.

During inspection, a flaw causes a very limited change in Φ and hence in Z or V_i . Typical values of such changes in detecting surface flaws are in the order of a few tenths of percent of

the quiescent value. Finite element studies indicate that the change in Φ caused by a deeply hidden flaw may be less than 0.01%. Therefore, it is very difficult to separate the change from the quiescent signal in the case of EC techniques.

The RFEC technique is based on the measurement of the voltage, V_i , induced in a pick-up coil by the flux, Φ_{RF} , which has passed the test object twice as shown in Figure 1. During inspection a flaw causes a significant change in Φ_{RF} and hence in V_i . The change in the phase of Φ_{RF} caused by a flaw has a linear relationship with the changes in the thickness of the pipe wall.

In conventional EC techniques, the probe lift-off has a significant effect on the impedance Z . In contrast, in the RFEC technique, lift-off alters the signal magnitude, but does not alter the signal phase significantly. Although the signal level of an EC probe is high, the perturbation caused by a flaw is small, i.e. the flaw-signal/quiescent-signal ratio is low. This limits the maximum gain that one can employ. In the case of RFEC techniques, although the signal level of the probe is low, the flaw-signal/quiescent-signal ratio is high. This allows higher gain levels to be used.

A super-sensitive eddy current system [5] has been developed to handle the extremely low amplitude signals obtained from RFEC probes. The total gain of such a system is about 40 dB higher than that of a conventional EC system.

An important consideration in designing the super-sensitive eddy current system is the requirement for the new system to be comparable with conventional EC system.

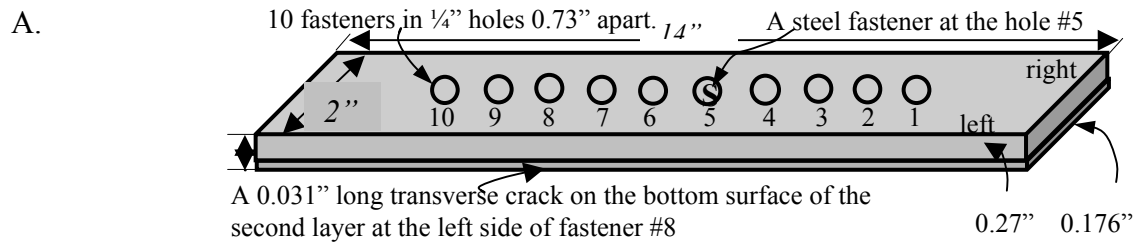
CURRENT STATUS OF RFECT FOR CRACK DETECTION

The system prototype has been tested using a number of specimens. The current test data¹ show that the system can detect: (1). aluminum material discontinuity 1.0" below the inspection surface; (2). a 12.7 mm x 12.7 mm x 0.15mm corrosion thinning 9.5 mm below the surface; (3). a 12.7 mm x 0.9 mm x 0.25 mm saw-cut 6.7 mm below the surface; and (4). a 0.78 mm long second layer fastener hole fatigue crack 11.3 mm below the surface, see Figure 3.

WING SPANWISE SPLICE STANDARDS

Two aircraft wing spanwise splice standards, provided by Boeing-St. Louis, contained first and second layer slots in fastener holes were used in the test. One standard had an aluminum wing skin/spar cap arrangement, each 0.125 inch thick, total thickness of about 0.25 inch, whereas the other had an aluminum skin/spar cap that was each 0.25-inch thick with total thickness about 0.5 inch. Slots were made in selected fastener holes located on both first and second layers of the two panels. Special attention was focused on the second layer slots. A description of the slots is provided in Tables 1 and 2. Figure 4 shows the fastener distribution and slot description for a portion of the area scanned in the Thick Panel. The test was carried out by Innovative Materials Testing Technologies, Inc. from December 2000 through January 2001. An older version, Version 2, of RF-4mm probe was used in the test.

¹ The test was done by using the newest version, Version 3, of probe RF4mm with the excitation-pickup coil separation of 29 mm.



B. **Detecting a 0.8 mm long 2nd layer fatigue crack 11.3 mm below surface: Real**

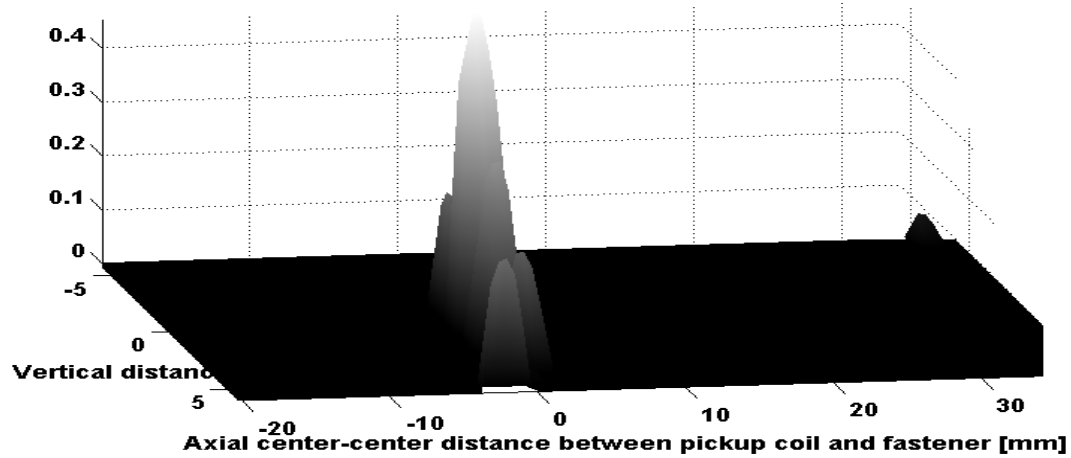


Figure 3. Detected slot signal with RFECT using a manually controlled scanner. A. Lockheed Georgia Specimen #B4-1; B. Detected slot signal, the normalized real component, with preset thresholds $X > 0$ and $Y > 0.1$.

Table 1. Description of Slots In the Thin Panel

Hole Number	1a + 1b	6-7	20	8	9-10	A	19	14-15	18
Fastener material	Al	Al-Fe	Fe	Fe	Fe-Fe	Al	Fe	Al	Al
Slot location	2 nd layer	2 nd layer	2 nd layer	2 nd layer	2 nd layer	1 st layer	2 nd layer	2 nd layer	2 nd layer
Slot Length inches	0.100+0.250	0.550	0.175	0.500	1.100	0.375	0.275	1.200	0.350
Detection	hit	hit	hit	hit	hit	hit	hit	hit	hit

Table 2. Description of Slots In the Thick Panel

Hole Number	1+1-2	4	A	7-8	12	13	14	15a-15b	16-17	18-19
Slot location	2 nd layer	2 nd layer	1 st layer	2 nd layer	2 nd layer	2 nd layer	2 nd layer	2 nd layer	1 st layer	2 nd layer
Fastener material	Al	Fe	Al	Fe-Fe	Fe	Fe	Al	Al	Al-Al	Al-Al
Slot Length inches	0.400+0.750	0.500	0.385	1.055	0.250	0.455	0.455	0.100+0.245	1.050	1.050
Detection	hit	hit	hit	hit	hit	hit	hit	hit	hit	hit

SCAN MODES

Manual A-scan with a guiding ruler was carried out for all scans. To obtain optimal detection results, to negotiate the populated aluminum and steel fasteners, and to minimize the influence from neighboring fastener hole signals, three different scan modes were applied during the slot detection. They are:

Mode 1, vertically oriented probe and axial scan.

Mode 2, axially oriented probe and axial scan;

Mode 3, angularly oriented probe and axial scan.

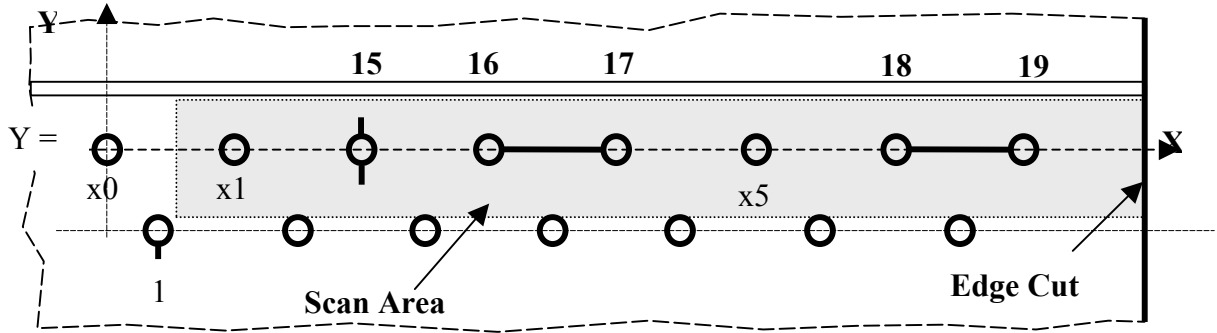


Figure 4. Schematic drawing showing typical fastener distribution and slot orientation for the Thick Panel

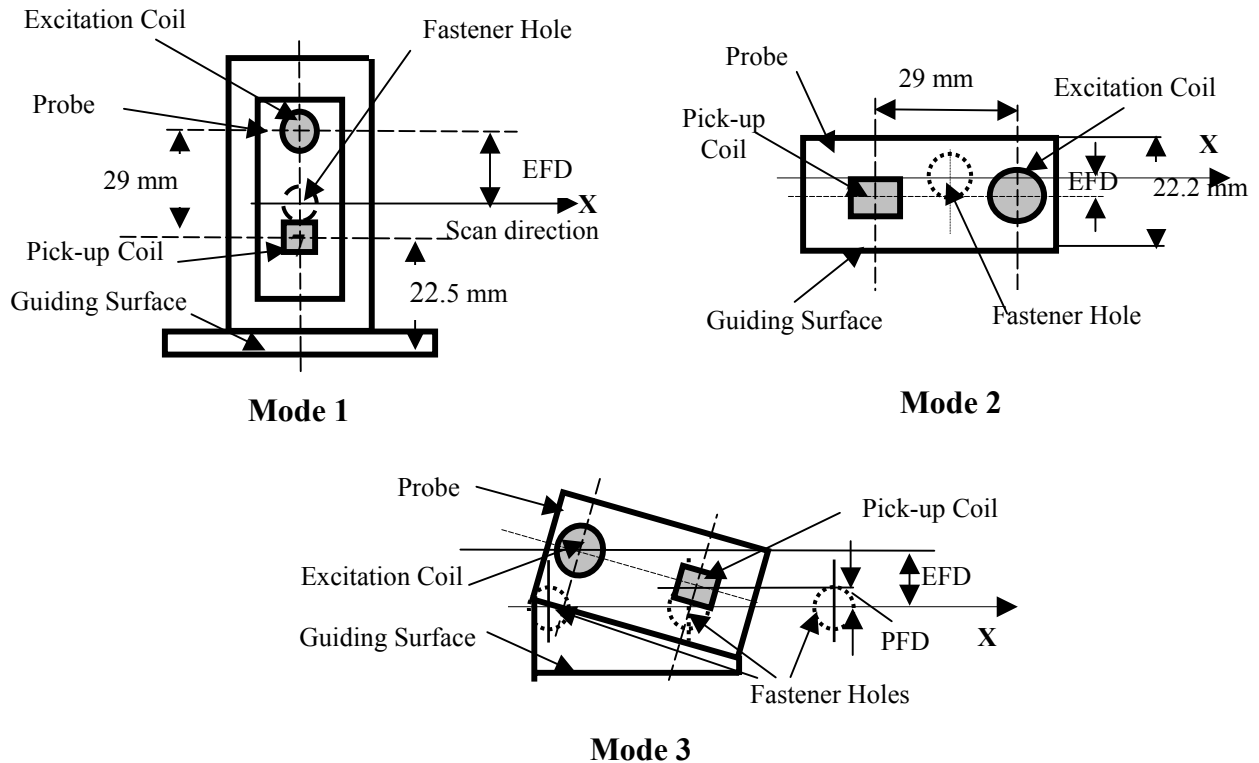


Figure 5. Description of the three scan modes

Mode 1 Non-Steel Fasteners

Mode 1 is the most sensitive scan mode. Both axially oriented and vertically oriented slots can be detected in this mode. Figure 6 shows a typical complex plane obtained using Mode 1 scan with the excitation-coil to fastener distance (EFD) = 19.7 mm and $f = 100$ Hz for scans shown in figure 4. Both the 2nd layer vertical slot on Hole #15 and the 1st layer axial slot between Holes 16 and 17 were detected. The 2nd layer axial slot between Holes 18-19 did not exhibit a significant response. However, it was detected using this mode with EFD = 32.5 mm and $f = 300$ Hz, see Figure 7.

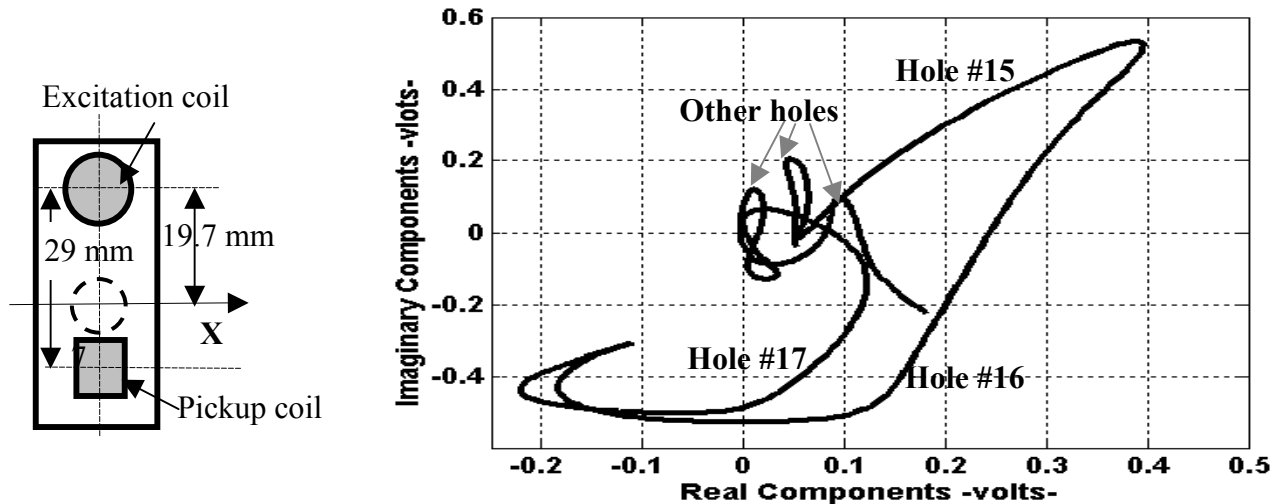


Figure 6. A typical complex plane obtained using Mode 1 with. EFD = 19.7mm

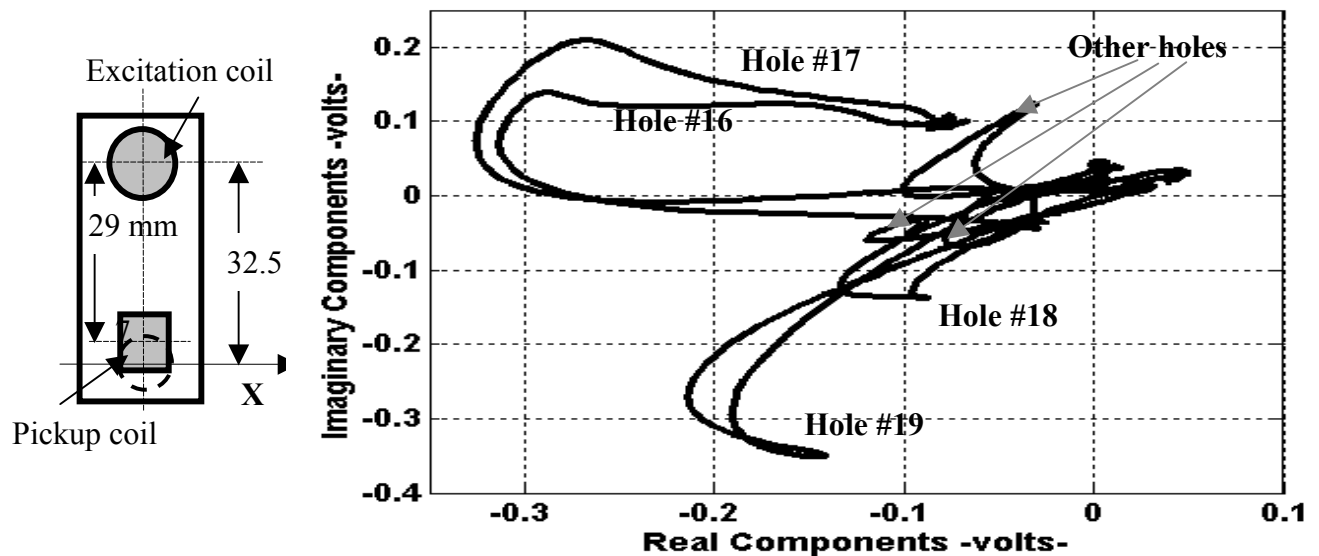


Figure 7. Complex plane obtained using Mode 1 with. EFD = 32.5 mm

The pickup-coil-to-slot-relationship should be noticed. A 2nd layer slot in a non-steel fastener hole is detected by an RFEC probe when an edge of its pickup coil is running over the slot.

Mode 1 Mixed Steel And Non-Steel Fastener Distribution

A steel fastener usually gives a very strong signal that may be several times magnitude of the signals obtained from a cracked non-steel fastener hole. Experience indicates that, for a mixed fastener case, the signals should be grouped separately where one group is for the steel fasteners and the other is for the non-steel fasteners. Figure 8 is an example of a mixed fastener distribution. Figure 9 shows the signals obtained at $f = 100$ Hz from an A-scan over fastener holes x1, 13, x2, 14 and x4. Only the two signals obtained from the two steel fastener holes, Holes x1 and 13, are significant. The signal from the slotted Hole 13 is very different from the non-slotted Hole x1 due to its phase angle.

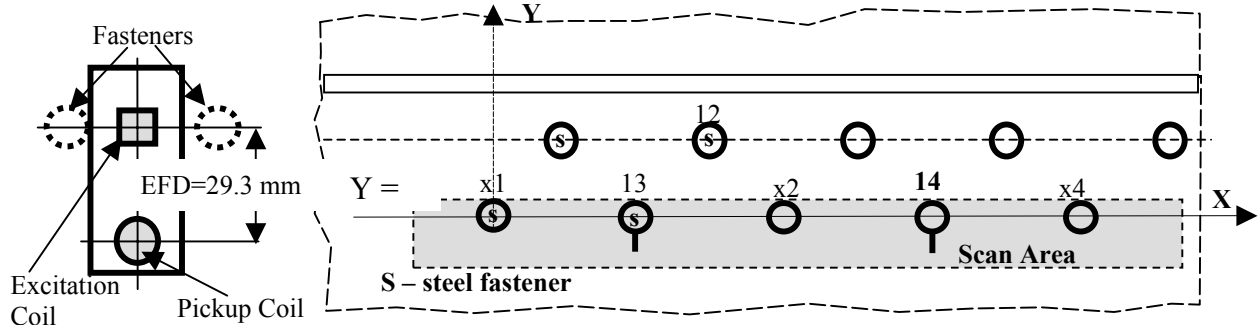


Figure 8. Schematic showing a scan area for a typical mixed fastener distribution (Thick Panel)

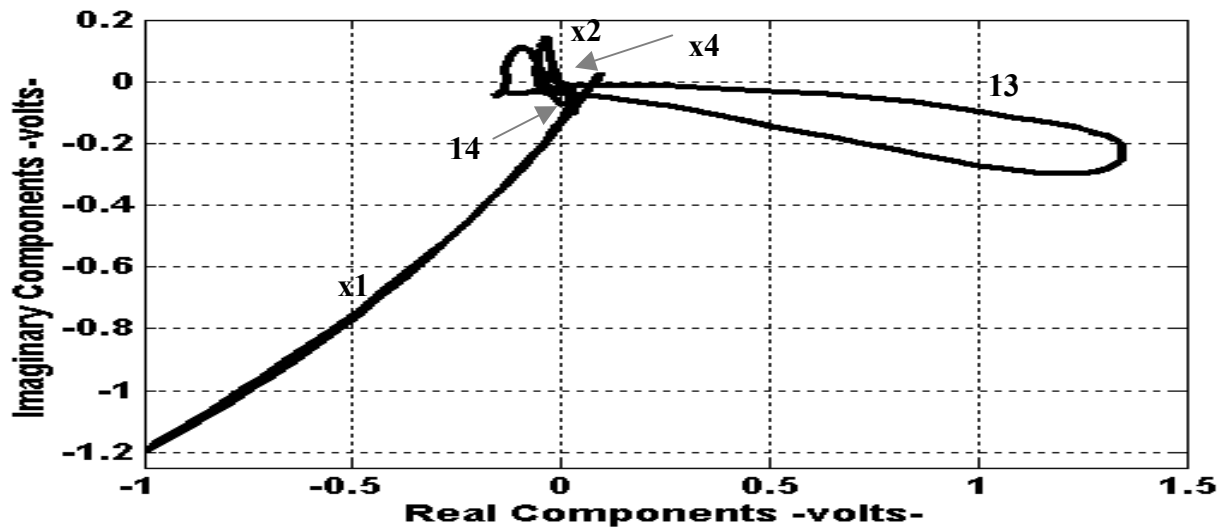


Figure 9. Complex plane obtained by scanning over a mixed fastener holes.

We could distinguish between the non-steel fastener Hole 14 and Holes x2 and x4 by removing the two steel fastener signals off the screen or to zoom in into a smaller area that includes only the non-steel fastener hole signals. However, in the current case, it would be even better if a higher frequency is applied to the probe. Figure 10 shows the signals obtained from an A-scan similar to that shown in Figure 9, but at $f = 500$ Hz and with the steel fastener signals excluded. The signal from the slotted hole, Hole 14, is different from those from non-slotted holes, Holes x2 and x4, by its magnitude and phase, while the phase difference is much more pronounced.

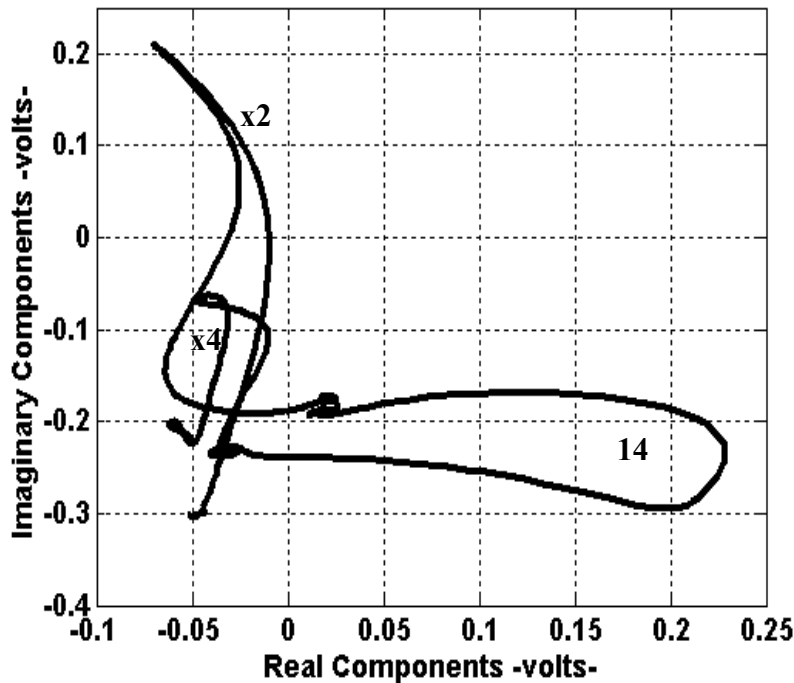


Figure 10. Responses obtained for $f = 500$ Hz.

A steel fastener may cause significant changes in the signals of its neighboring fasteners holes which may confuse an operator. However, it has been found that there is an effective way to minimize this effect by placing the pickup coil of a probe away from all steel fasteners. As an example, Figure 11 shows a section of the Thick Panel where an axial slot is present in Hole #4 with a steel fastener. The fasteners in the two neighboring holes are steel also. Huge signals would be obtained in an RFEC probe if the pickup-coil-to-slot relationship was similar to that shown in Figures 7, 8 and 9.

Figure 11 and 12 depict a solution to this problem. The pickup coil is placed away from the fastener holes. Figure 13 shows the 300 Hz signal from Hole 4 that is clearly distinguished from the signals from other holes.

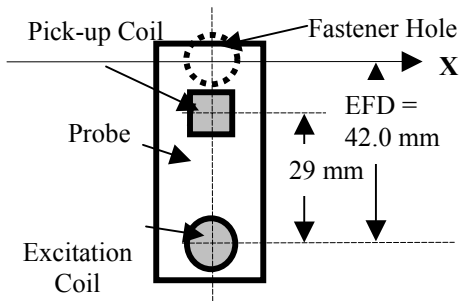


Figure 11. Arrangement for improving response from holes with steel fasteners

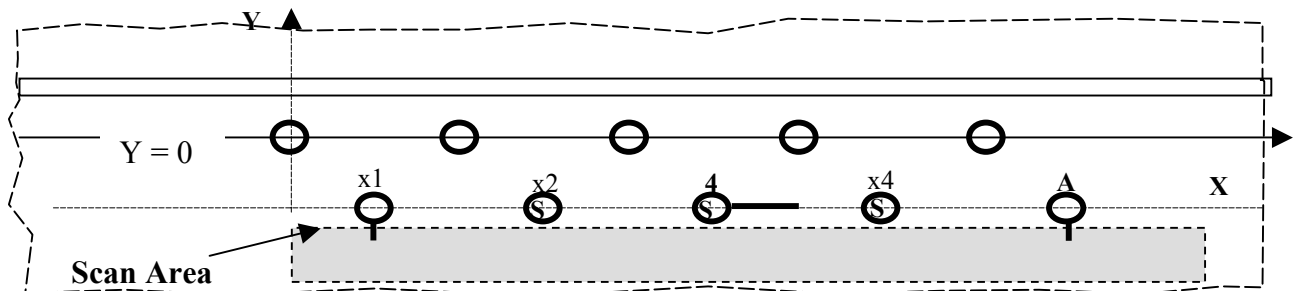


Figure 12. Schematic drawing showing scan area with adjacent steel fasteners.

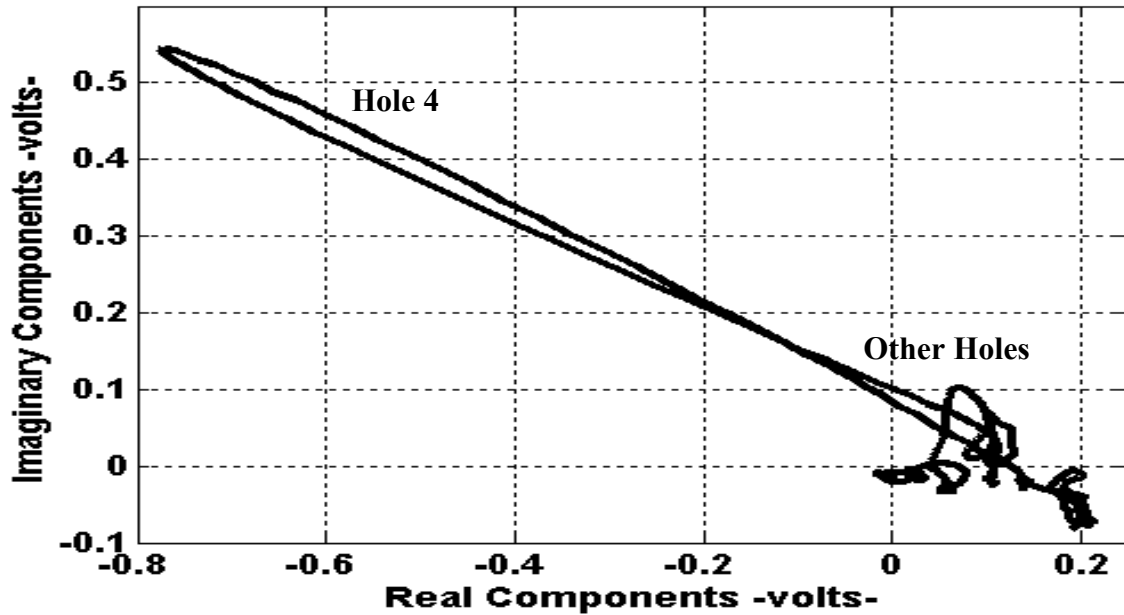


Figure 13. Signals from Hole 4 with a steel fastener in the hole and two steel fasteners in the neighboring holes.

Mode 2 Non-Steel Fasteners

In practice, Mode 1 may not always be possible because of the geometrical restriction from neighboring holes as well as other structural factors. In the case when Mode 1 is not possible Mode 2 can be applied. Figure 14 shows the complex plane obtained using Mode 2 scanning over holes 15, 16-17 and 18-19, see Figure 4, with EFD = 14.3 mm and $f = 100$ Hz. The signal from Holes 18-19 is different from other signals in its phase and magnitude.

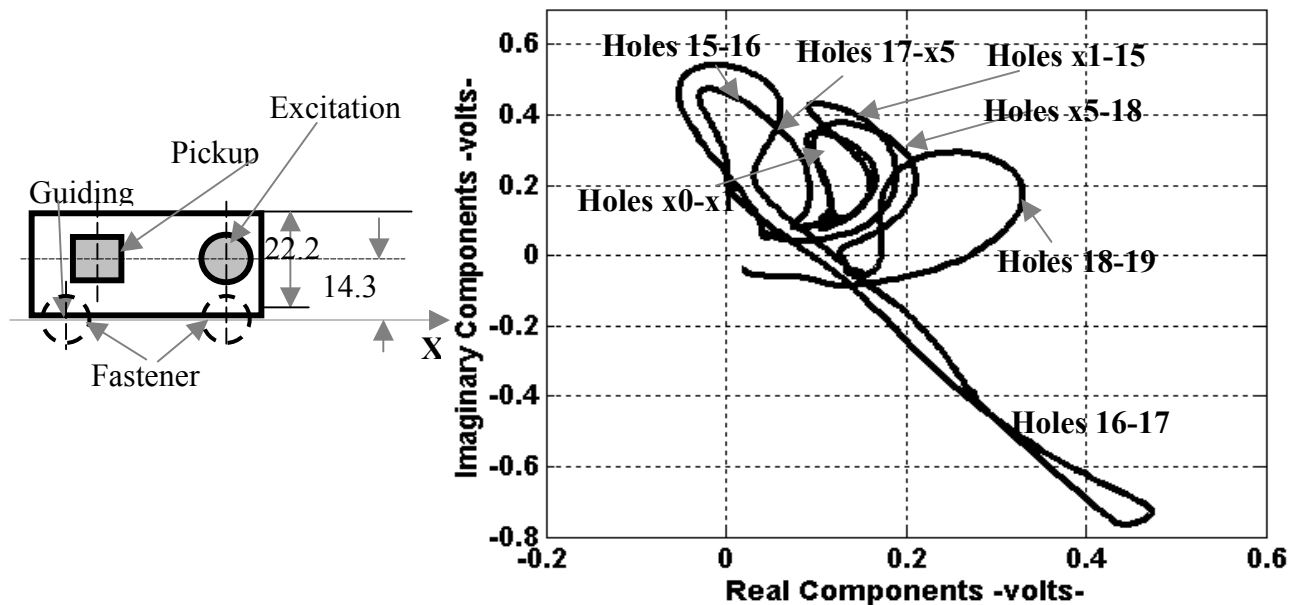


Figure 14. Complex plane obtained using Mode 2 scanning over holes 15, 16-17 and 18-19. EFD = 14.3 mm

Mode 2 Detecting Slotted Holes Among Steel Fasteners

The best way to detect a slotted hole among steel fasteners is to place the pickup coil of a probe away from the fastener holes. Figure 15 is an example of the probe arrangement used to scan. Figure 16 is an example of an axial slot connecting steel fastener holes, Holes 7 and 8.

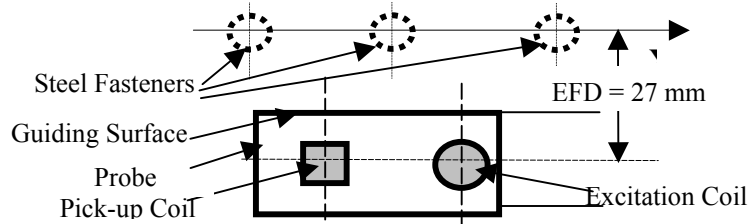


Figure 15. Probe arrangement for scanning steel fastener holes, Holes 7 and 8.

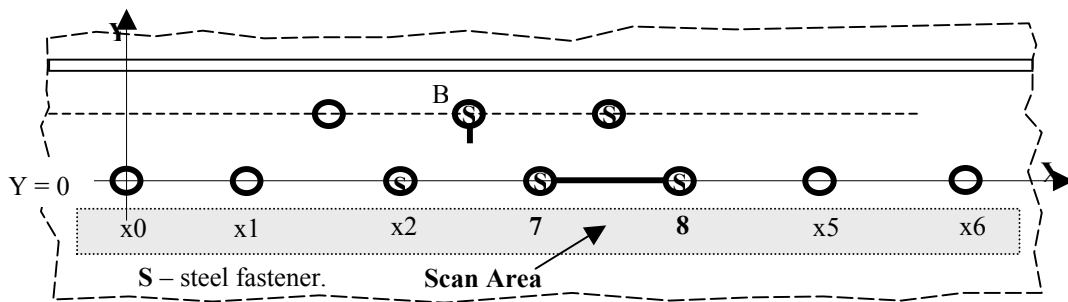


Figure 16. Schematic drawing showing location of axial slot between Holes #7 and 8 among steel fasteners.

Figure 17 shows the slot signal between Holes 7 and 8 at $f = 100$ Hz. It is easily distinguished from other signals although among the six signals three are affected either by the slot or by the steel fastener in Hole x_2 . Figure 18 illustrates each signal separately for comparison.

Mode 3 Detecting Slots On Steel And Non-Steel Fastener Holes

A major disadvantage of applying Mode 2 is that, while the pickup coil of a probe passes over a fastener hole, the excitation coil is also close to a neighboring hole and receives a signal from that hole. This means any slot and any steel fastener has its impact on signals twice. This is acceptable if there is only a single slotted hole or a single steel fastener. However, in the case of Figure 14, five of the eight holes are slotted holes. Each slotted hole exhibited two responses. As a result all signals, but that of Holes x_0 - x_1 , are affected by a slot. In this case Mode 3, see Figure 5, can be made of use.

Mode 3 can be an improvement of Mode 2. It reduces the influence caused by the excitation coil signal. The mode was using in detecting first and second layer slots in the Thin Panel. The results are not shown due to the space limitation of the paper.

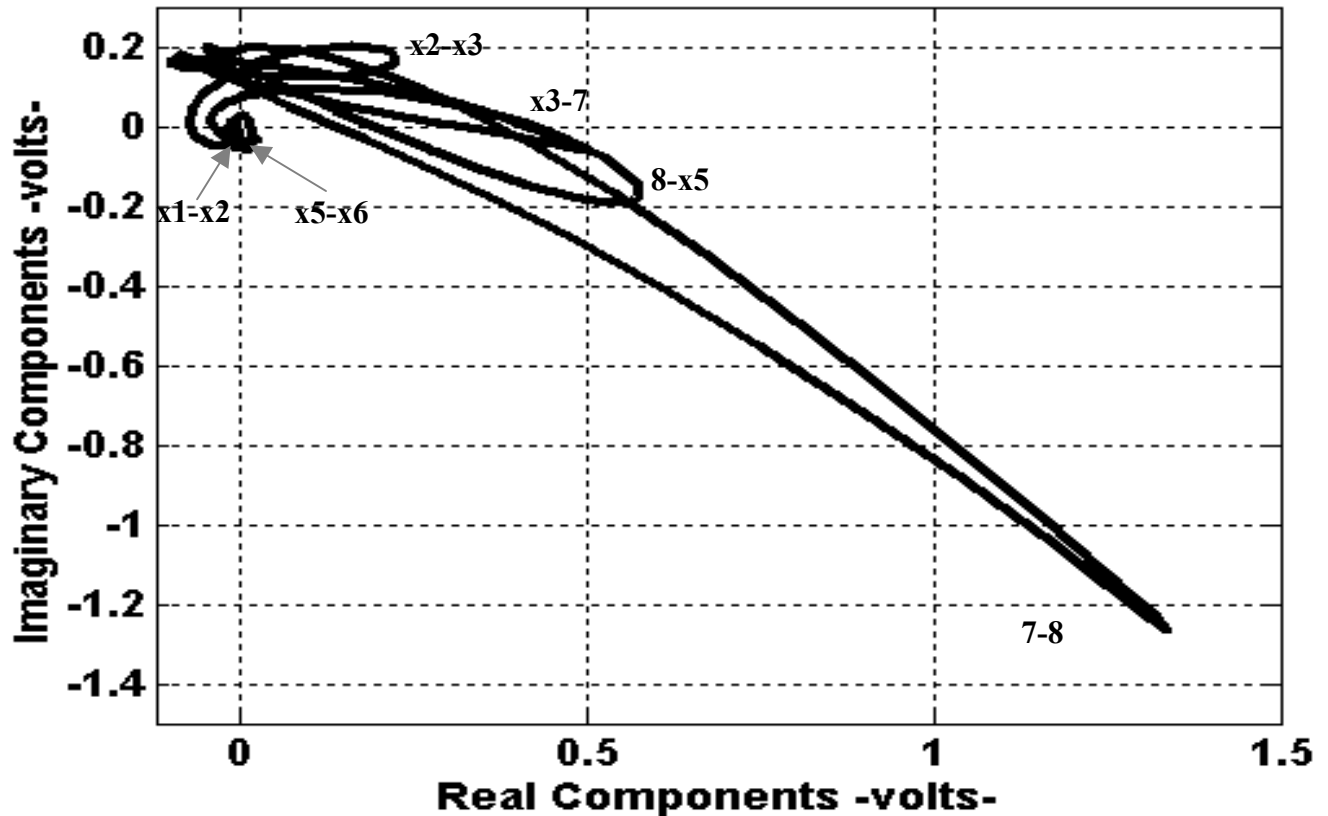


Figure 17. Signals from Mode 2 scanning over the holes shown in Figures 16. EFD = 27 mm.

CONCLUSIONS

1. The first and second layer slots in the two wing spanwise splice standards were detected using the RFEC technique.
2. Three different scan modes were used to perform the tasks. While Mode 1, axially oriented probe and vertical scan, provides the best sensitivity to slots, Mode 2 and Mode 3 provide better flexibility in negotiating a probe among fastener holes and other structure restrictions.
3. Preliminary results include:
 - To detect a slotted hole with a non-steel fastener the RFEC probe should be positioned with one edge of its pickup coil close or right on top of the slot.
 - To detect a slotted hole with a steel fastener the pickup coil should be placed away from the slotted hole, as well as away from other steel fasteners.
 - To detect a slotted hole within a mixed fastener distribution it is necessary to separate the signals into two groups, one is for those obtained from non-steel fastener holes; the other is for steel fastener hole signals. The analysis of the signals should be carried out separately in two different groups also.

For second layer slots a slotted hole signal is different from a non-slotted hole signal in both its magnitude and phase angle, but the phase angle has the more pronounced difference.

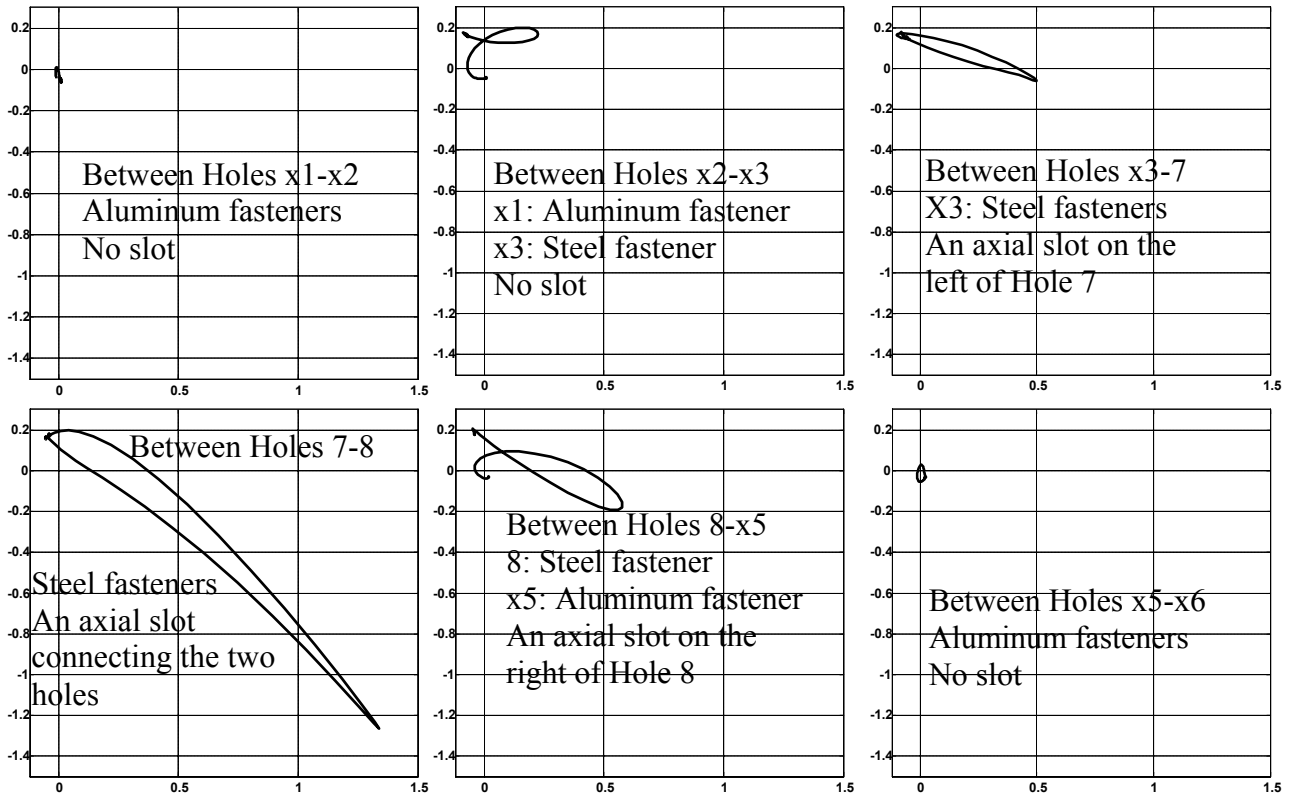


Figure 18. Individual signals from holes shown in Figure 17.

REFERENCES

- [1]. Lord, W., Sun, Y., Udpa, S., A Finite Element Study of the Remote Field Eddy Current Phenomenon, *IEEE Transaction on Magnetics*, Vol. 24, PP. 435-438, January 1988.
- [2]. Sun, Y.-S, Finite-Element Study of Diffusion Energy Flow in Low-Frequency Eddy Current Field, *Materials Evaluation*, 47/1 (1989) 87-92.
- [3]. Sun, Y., US Patent #6,002,251, *Electromagnetic-field-focusing remote-field eddy current probe system and method for inspecting anomalies in conducting plates*, December 14, 1999.
- [4]. Sun, Y.S, Ouyang, T., and Udpa, S., "Remote Field Eddy Current Testing: One of the Potential Solutions for Detecting Deeply Embedded Discontinuities in Thick and Multilayer Metallic Structures", *Materials Evaluation*, 59/5 (2001) 632-637.
- [5]. Ouyang, T., US Pending, US Patent Application Serial No. 09/540,370, *Super-Sensitive Eddy Current System And Method*, filed on March 31, 2000.